

SPECTROSCOPIC AND PHOTOMETRIC ANALYSIS OF THE WN7 ECLIPSING BINARY CQ CEPHEI

KAM-CHING LEUNG

Department of Physics and Astronomy, Behlen Laboratory of Physics, University of Nebraska-Lincoln

ANTHONY F. J. MOFFAT¹

Département de Physique, Université de Montréal

AND

WILHELM SEGGEWISS

Observatorium Hoher List der Universität Bonn

Received 1982 January 4; accepted 1982 August 11

ABSTRACT

Spectroscopic observations taken at Kitt Peak in 1978 September are used to analyze the orbit of the WN7 eclipsing binary CQ Cep. In general, the Wolf-Rayet emission lines and their violet-displaced absorption edges display a circular orbit with a velocity amplitude (semiamplitude) of 310 km s^{-1} (N IV $\lambda 4058$ emission) in the photometric 1^d64 period.

The violet-displaced hydrogen Balmer absorption lines vary in phase with the W-R emission, indicating that they originate in the W-R atmosphere rather than in the unseen companion star. The He II $\lambda 4686$ emission shows a heavily distorted velocity curve as was already noted for the 1941-1943 observations by Hiltner. The violet-displaced absorption component of the He I $\lambda 3889$ line shows a nearly constant velocity of about 1150 km s^{-1} , indicating its origin in a common binary system envelope.

The 1947 photoelectric observations of Hiltner were analyzed employing the Wilson and Devinney approach. The behavior of the secondary maximum of CQ Cep is very similar to the case of UW CMa. A series of solutions was obtained by assuming different values for the mass ratio. Since the detection of the secondary spectrum is in doubt, this sets a limit on the differential brightness between the components. This in turn leads to an upper limit on the mass ratio, $q = m_O/m_{W-R}$. The possible mass range for the WN7 component sets a lower limit on q . With the two constraints q was found to lie close to 0.75. The system CQ Cep was found to be in contact with about 50% overcontact. Limits on the absolute dimensions were also obtained. Physical interpretations of CQ Cep are discussed.

Subject headings: stars: eclipsing binaries — stars: individual — stars: Wolf-Rayet

I. INTRODUCTION

In the fourth part of the series on Wolf-Rayet stars of spectral type WN7 (Moffat and Seggewiss 1979) we discussed the relation of the WN7/WN8 stars to the other W-R stars and their distribution and kinematics in the Milky Way system. The scarcity of fundamental physical data of WN7 stars, like masses, temperatures and radii, prompted us to initiate new spectroscopic observations of prominent members of that luminous group of W-R stars.

CQ Cep (HD 214419, $\alpha[1900] = 22^h 32^m 9, \delta[1900] = +56^\circ 23'$) is the only eclipsing binary known among the WN7/WN8 stars. It has the shortest orbital period of any known W-R binary.

¹Visiting Astronomer, Kitt Peak National Observatory, which is operated by the Association of Universities for Research in Astronomy, Inc., under contract with the National Science Foundation.

McLaughlin and Hiltner (1941) announced the star to be a spectroscopic binary, and Hiltner (1944) derived a first spectroscopic orbit. He determined circular elements from the N IV emission line at 4058 \AA which he found to vary little in intensity. He already noted that the velocities of the violet-displaced absorption edges of the He II Pickering series vary in phase with their emission counterparts and that the absorption edges of He I $\lambda\lambda 4471, 4026,$ and 3889 are often split into two components. The He II $\lambda 4686$ emission showed a unique radial velocity curve with high eccentricity and reduced velocity amplitude together with appreciable variations in structure and intensity.

Bappu and Visvanadham (1977) also obtained radial velocity curves for the N IV $\lambda 4058$ and He II $\lambda 4686$ emission lines. They stressed that N IV $\lambda 4058$ was the best line to obtain the W-R star orbit, while He II $\lambda 4686$ might be formed partly in a common envelope.

Another N IV $\lambda 4058$ radial velocity curve was obtained by Niemela (1980). She also published a velocity curve for an absorption feature discovered on top of the very strong He II $\lambda 4686$ emission. This feature was claimed to arise in a companion star, whereas this and other companion star lines never have been seen before.

Gaposchkin (1944) discovered that CQ Cep is an eclipsing binary. Photoelectric light curves were first measured by Hiltner (1950) in broad-band spectral regions centered near 3550 and 5300 Å and, after prismatic dispersion, in the light of the He II $\lambda 4686$ emission. Hiltner deduced that the He II light curve excludes an origin of the emission in a compact shell around the W-R star as well as its origin in a large envelope.

The light curve of CQ Cep has been frequently obtained by Soviet observers: Tchugainov (1960), Gusseinzade (1969), and Kartasheva (1972) used broad-band photoelectric photometry similar to the *UBV* system; Khaliullin and Cherepashchuk (1970), Khaliullin (1972) and Kartasheva (1976) used narrow-band photometry. Kartasheva and Svechnikov (1974) tried to divide the light curve into a stellar and a shell component.

Times of minima of CQ Cep from 1901 to 1967 have been discussed by Semeniuk (1968). She computed the ephemeris

$$\text{JD}(\text{Min } I) = \text{JD } 2,432,456.668 + 1^d 641245 E,$$

which is superior to all trials of improvement by radial velocity curves.

Hiltner and Schild (1966) classified CQ Cep as WN7-A based on their criteria of "relatively narrow lines, strong continuum, and ... absorption lines characteristic of O-B stars." The spectral type of the star given by Smith (1968) is WN7+O7. However, one should be aware that the Balmer absorption lines might arise in the W-R star itself as is the case for HD 92740, of type WN7 (Moffat and Seggewiss 1978).

II. SPECTROSCOPIC OBSERVATIONS AND REDUCTIONS

The star was observed by A. F. J. M. in 1978 September with the white spectrograph attached to the No. 1 90 cm telescope of the Kitt Peak National Observatory. Twenty-six spectrograms were obtained on nitrogen-baked IIIa-J plates behind a Carnegie image tube. The mean exposure time was 4 minutes. The linear reciprocal dispersion is about 42 \AA mm^{-1} . A journal of observations is given in the first two columns of Table 1.

The spectra were measured by W. S. using the modified digitalized Abbe comparator of the Hoher List Observatory. The derived radial velocities (RV) are listed in Table 1. Comments on individual lines follow.

N IV $\lambda 4058$. This is a symmetric, moderately weak, relatively sharp emission line. Of any line, its velocity

probably serves best to give the systemic velocity of the binary system as was pointed out by Bappu and Visvanadham (1977) and shown for a complete sample of WN7/8 stars by Moffat and Seggewiss (1979).

N V $\lambda 4604$. Both the emission and the violet-displaced absorption components have been measured with some confidence. The $\lambda 4620$ line of the N V doublet gives a large RV scatter because of blending with N III $\lambda \lambda 4634, 4641, 4642$ and is therefore not listed here. The N III multiplet itself is too asymmetric to be measured. The other strong N III multiplet blend at $\lambda \lambda 4097, 4103$ is severely affected by He II and Si IV.

He II $\lambda 4686$. This is the strongest emission feature in the visual part of the spectrum. It has no violet-displaced absorption edge but its blue side is reduced in intensity between phases 0.5 and 1.0. We do not see evidence for unshifted $\lambda 4686$ absorption as claimed by Niemela (1980) in her spectra.

He II $\lambda 4542$. Emission and absorption components were safely measured. In addition, He II $\lambda 4339$ (+H γ) and He II $\lambda 4200$ were measured, but their RV scatter is very large.

He I $\lambda 3889$. The He I emission was measured with difficulty due to its weakness and asymmetry. However, its violet-displaced absorption is present in all spectra. Intensity and shape of the line are highly variable. Half of the spectra show a weak second absorption component. Also, the violet-shifted absorption edges of the He I $\lambda 4472$ line are normally split into two components. The splitting of both He I absorption lines was already noted by Hiltner (1944).

H9 $\lambda 3835$. The higher Balmer series ($\geq H8$) can be detected in all well-exposed spectra, but only H9 could be measured with confidence.

Interstellar lines. The Ca II lines are prominent. Their mean radial velocities are:

$$\text{Ca II H} - 34 \pm 13 \text{ km s}^{-1} \text{ (s.d.)}$$

and

$$\text{Ca II K} - 24 \pm 8 \text{ km s}^{-1} \text{ (s.d.)}.$$

The diffuse interstellar band at $\lambda 4430$ was detected in some spectra but was too weak for measurement.

III. DISCUSSION OF THE SPECTROSCOPIC RESULTS

All radial velocities have been plotted versus phase of the eclipsing system (Figs. 1-5). The phases (see Table 1, col. [3]) have been computed from Semeniuk's (1968) ephemeris which is based on 66 years of light curve minima (see § I).

All RV plots except those of He II $\lambda 4686$ emission and He I $\lambda 3889$ absorption can be adequately represented by sine functions indicating a circular orbit of the binary system. Formal eccentric orbit fits to the best

TABLE 1
RADIAL VELOCITIES (km s^{-1}) OF LINES IN THE SPECTRUM OF CQ CEPHEI (HD 214419)

PLATE (1)	JD(Hel): 2,443,700 (2)	PHASE (3)	N IV 4058		N V 4604		He II 4686		He II 4542		He I 3889 Abs. (10)	H9 Abs. (11)
			Em. (4)	Em. (5)	Abs. (6)	Em. (7)	Em. (8)	Abs. (9)				
4833d	68.6724	0.331	-334	-1	-439	-29	-160	-507	-1100:	
4834a	68.7516	0.380	-228	+62	-374	-23	-75	-499	-1113:	-377	-377	
4834f	68.7981	0.408	-212	+29	-344	-7	+33	-481	-1266	-380	-380	
4835b	68.8453	0.437	-194	+65	-308	-4	-37	-474	-1112	-456	-456	
4835e	68.8932	0.466	-129	+117	-245	+10	+127	-391	-1121	-241	-241	
4836a	68.9481	0.499	-51	+179	-139	+31	+157	-380	-1117	-191	-191	
4836e	69.0037	0.533	-13	+215	-96	+45	+224	-217	-1141	-186	-186	
4837d	69.6571	0.931	+65	+234	-188	+121	+214	-194	-1115	-106	-106	
4837g	69.7058	0.961	+12	+184	-197	+72	+199	-281	-1168	-186	-186	
4838a	69.7294	0.975	+27	+99	-258	...	+145	-355	-1156	
4839c	69.8162	0.028	-150	+36	-317	+18	+46	-357	-1205	-374	-374	
4839g	69.8808	0.068	-195	-57	-392	-34	+40	-448	-1194:	-203	-203	
4840d	69.9544	0.112	-274	-45	-476	-47	-14	-445	...	-479	-479	
4840g	69.9849	0.131	-335	-98	-467	-42	-54	-507	-1224:	-477	-477	
4841d	70.6586	0.542	+38	+264	-144	+47	+232	-194	-1044	-90	-90	
4841g	70.7113	0.574	+76	+307	-103	+121	+395	-199	-1110	-264	-264	
4843a	71.6002	0.115	-306	-95	-453	-74	-24	-506	-1145	-445	-445	
4843g	71.7120	0.183	-372	-137	-475	-25	-141	-505	-1171	-587	-587	
4845c	71.8197	0.249	-351	-103	-476	-40	-188	-542	-1209	
4845g	71.9287	0.315	-327	-81	-460	-30	-156	-506	-1030	-512	-512	
4846d	71.9919	0.345	-272	-6	-418	-28	-116	-535	-1181	-448	-448	
4847a	72.6016	0.725	+242	+442	+147	+307	+523	-3	-1125	+40	+40	
4847g	72.7093	0.791	+191	+439	+83	+272	+440	-18	-1142	-63	-63	
4848f	72.7815	0.835	+208	+376	+46	+269	+417	-4	-1163	-90	-90	
4849g	72.8614	0.884	+158	+321	-36	+235	+236	-104	-1130	-110	-110	
4850e	72.9593	0.943	+96	+248	-240	+91	+215	-161	-1160	-222	-222	

line, N IV $\lambda 4058$, yield $e = 0.08 \pm 0.02$ for the present data, while Bappu and Visvanadham (1977) give $e = 0.04 \pm 0.02$. In view of the short period and the light curve perturbations, we assume these small eccentricities to be fictitious and that the orbit is really circular. In any case, the pseudoeccentricity of the curves can be easily accounted for by tidal distortion, reflection effect, and eclipses in a circular orbit (cf. Fig. 1). The velocity amplitudes (semiamplitudes), mean velocities, and differences O - C from the ephemeris, as well as values for N IV from other sources, are given in Table 2. The quality of the measurements can be estimated from the standard deviation of a single velocity from the sine fit given in the last column of Table 2.

The line of best quality is the N IV $\lambda 4058$ emission. Our amplitude of $310 \pm 7 \text{ km s}^{-1}$ from the RV curve is compared with Hiltner's (1944) value of 295 km s^{-1} and our mean velocity of $-60 \pm 5 \text{ km s}^{-1}$ with his value of -75 km s^{-1} . The agreement is good in view of the difficulty of measuring broad W-R emission lines. Both values of the mean velocity are compatible with the expected radial velocity component of galactic rotation plus solar motion, -60 km s^{-1} , given for CQ Cep by Moffat and Seggewiss (1979).

From the same line we derive the mass function:

$$f(m) = \frac{(m_2 \sin i)^3}{(m_1 + m_2)^2} = 5.08 \pm 0.34 m_{\odot},$$

where m_1 is the mass of the W-R star and m_2 the mass of its companion. Also we have the separation

$$a_1 \sin i = 10.1 R_{\odot}.$$

The RV curves of the following four lines deserve special attention:

H9 $\lambda 3835$. The curve of this line (Fig. 1, lower), which is representative of the hydrogen Balmer absorption, is exactly in phase, and the velocity amplitude is comparable with the W-R emission. Therefore, we must conclude that the hydrogen absorption originates in the W-R atmosphere as is observed also for the WN7 star HD 92740 (Moffat and Seggewiss 1978; Conti, Niemela, and Walborn 1979). The mean H9 velocity of 261 km s^{-1} is of the order of the mean velocities of the violet-displaced absorptions which indicates a common place of formation in the expanding W-R envelope.

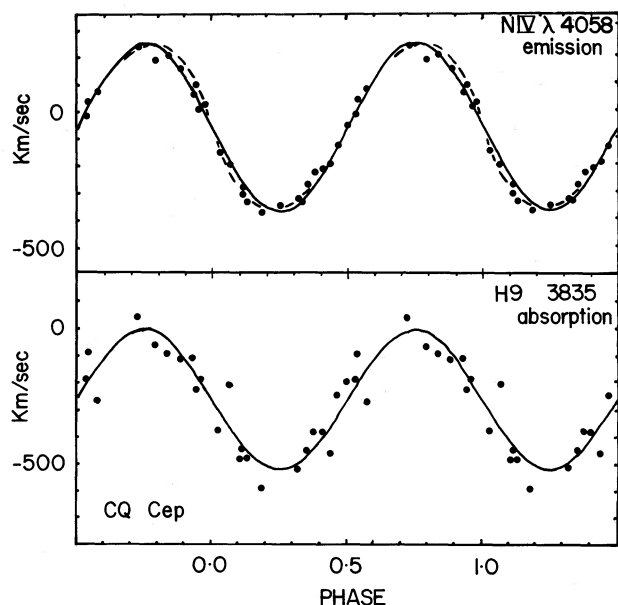


FIG. 1.—Radial velocity curves of CQ Cep for the lines N IV λ 4058 (emission) and H9 λ 3835 (absorption). The solid lines represent best sine fits. Primary light minimum occurs at phase zero when the WN7 component is behind. The broken curve refers to theoretical radial velocities assuming a circular orbit as shown by the solid curve with elements from Table 2, but including total distortion reflection effects and eclipses (cf. Wilson and Sofia 1976) according to the light curve in Table 4 with $q=0.75$. Calculations for other (noisier) lines yield similar results and are not shown.

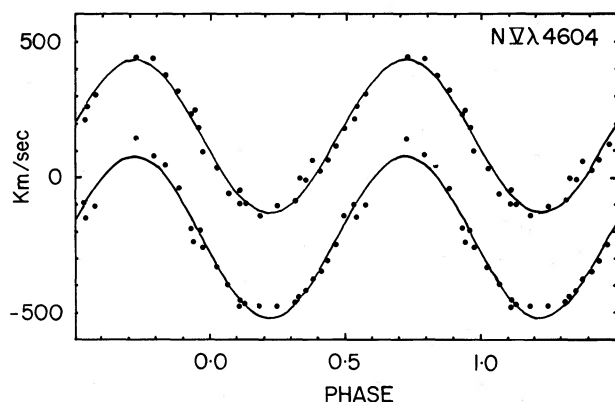


FIG. 2.—Radial velocity curves of CQ Cep for the emission (*upper*) and violet-displaced absorption (*lower*) component of the line N V λ 4604. The solid lines represent best sine fits.

He II λ 4686. The RV curve (Fig. 4) is heavily distorted in comparison to the sine curves of the other lines. As Hiltner (1944) already noted, He II λ 4686 may not represent the true orbital motion because “this line is subject to appreciable variations in structure during a cycle.” It is most remarkable that the structural changes of the 1978 observations, e.g., the reduction of the

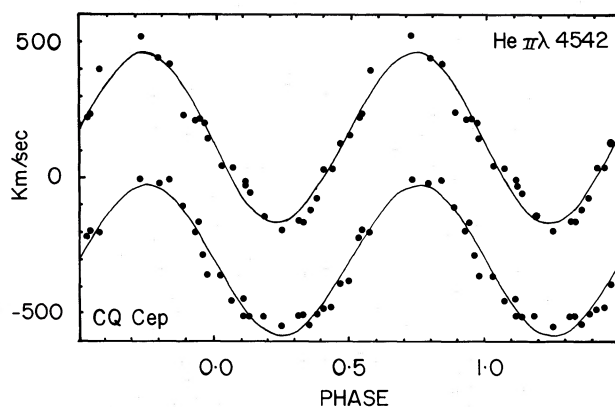


FIG. 3.—Radial velocity curves of CQ Cep for the emission (*upper*) and violet-displaced absorption (*lower*) component of the line He II λ 4542. The solid lines represent best sine fits.

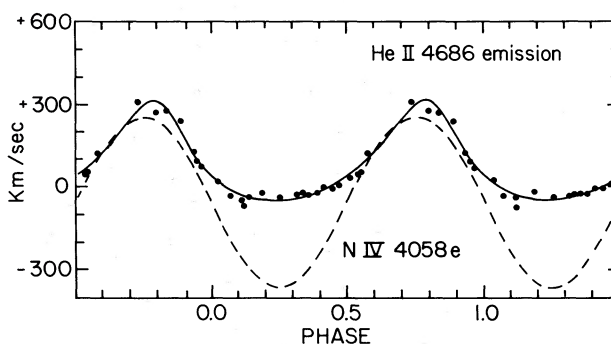


FIG. 4.—Radial velocity curves of CQ Cep for the emission line He II λ 4686 with the solid curve derived from the elements of Table 3. The dashed line is the orbit from N IV λ 4058.

emission to the blue between phases 0.5 and 1.0, appear still in the same manner as in Hiltner's 1941–1943 observations. Hypothetical elements of a fictitious elliptical orbit (Table 3) of our observations are still in fair agreement with the elements derived by Hiltner (1944) from a rough graphical solution, as well as the elements of Bappu and Visvanadham (1977). The distortion of this strong line may be related to the fact that at least part of the He II λ 4686 emission originates in the hot zone between the stars (cf. § V).

He I λ 4472. In Figure 5 (*upper*) we have plotted the velocities of two components of the violet-displaced absorption edges of this low-excitation line. While the amplitude remains like that of the emission lines, there is a major phase shift of 0.30. This probably implies streaming motions similar to those seen especially in low-excitation lines of other W-R stars, e.g., in θ Mus (Moffat and Seggewiss 1977). Such lines are formed in the outer regions of the envelope.

He I λ 3889. The velocities of the violet-displaced absorption edges for two components are plotted in

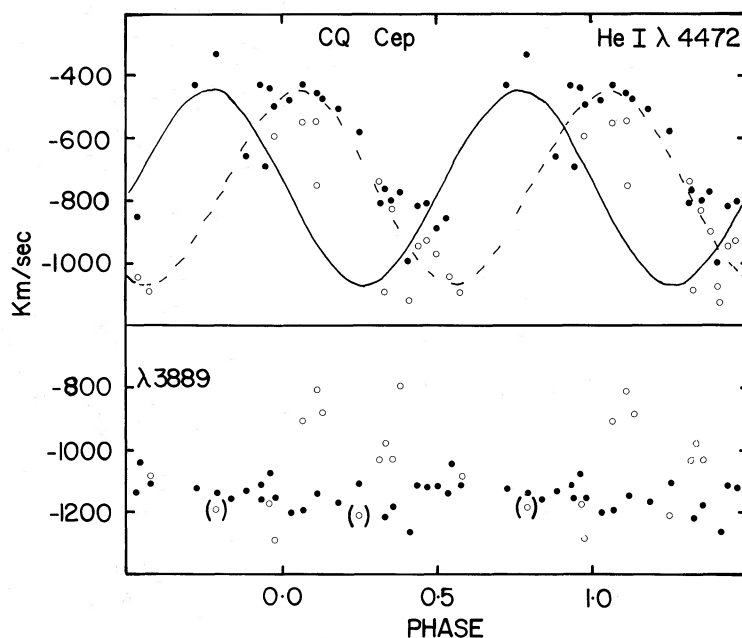


FIG. 5.—(Upper): Radial velocity curve of CQ Cep for the violet-displaced absorption components of the line He I $\lambda 4472$ (solid circles, main line component; open circles, secondary line component). The solid curve refers to N IV $\lambda 4058$ as in Fig. 1 but shifted in velocity by 700 km s^{-1} ; the dashed curve is the same line but shifted also in phase by 0.30 to match the observations. (Lower): As above but for He I $\lambda 3889$ and without the N IV $\lambda 4058$ curve.

TABLE 2
ORBITAL ELEMENTS OF CQ CEPHEI (HD 214419)

Line	Type or Source	Velocity Amplitude (km s^{-1})	Mean Velocity (km s^{-1})	Phase Shift (O-C)	Standard Deviation (km s^{-1})
N IV $\lambda 4058$	Emission	310 ± 7	-60 ± 5	0.004 ± 0.020	± 26
N V $\lambda 4604$	Emission	280 ± 10	$+153 \pm 6$	0.028 ± 0.029	± 31
	Viol. displ. abs.	299 ± 8	-220 ± 9	0.029 ± 0.022	± 33
N V $\lambda 4620$	Viol. displ. abs.	250 ± 12	-233 ± 8	0.022 ± 0.037	± 51
He II $\lambda 4542$	Emission	312 ± 13	$+148 \pm 8$	0.013 ± 0.034	± 42
	Viol. displ. abs.	276 ± 10	-303 ± 6	-0.002 ± 0.024	± 41
H9 $\lambda 3835$	Absorption	257 ± 18	-261 ± 12	0.009 ± 0.056	± 68
N IV $\lambda 4058$ emission ...	Hiltner 1944	295	-75
	Bappu and Visvanadham 1977	295	-62
	Niemela 1980	285	-85

NOTE.—Orbital elements are derived from various spectral lines with period $P = 1^d641245$ and initial epoch $T_0 = \text{JD } 2,432,456.668$ according to Semeniuk 1968; circular orbit assumed. Values are also given for N IV $\lambda 4058$ from other sources.

Figure 5 (lower). The stronger one varies about a mean value of $-1150 \pm 52 \text{ km s}^{-1}$ (s.d.). Evidently this component of the line does not take part in the binary motion. We may conclude that it originates in an expanding envelope common to both stellar components of the binary system CQ Cep. This is to be expected if the feature is the outermost one, reaching about 5 times

the WN7 core radius (cf. Underhill 1969), i.e. $\sim 50 R_{\odot}$ which is larger than the orbital separation (cf. Table 4B). The secondary component of the line appears to vary like He I $\lambda 4472$ but with reduced amplitude and increased phase shift. In view of the near antiphase variation relative to N IV $\lambda 4058$, one might suspect that this component arises in the companion O-star, as claimed

TABLE 3
HYPOTHETICAL ELEMENTS FOR A FICTITIOUS ELLIPTICAL ORBIT OF CQ CEPHEI (HD 214419)

Element	Hiltner 1944	Bappu and Visvanadham 1977	This Paper
Period, P (days)	1.6410	1.6413	1.641245
Velocity amplitude, K (km s ⁻¹)	165	148	181 ± 8
Mean velocity, γ (km s ⁻¹)	137	118	77 ± 5
Periastron passage, T_0 (JD [Hel])	2,443,772.736 ± 0.076
	(Phase 0.75)	...	(Phase 0.81)
Eccentricity, e	0.35	0.31	0.29 ± 0.04
Longitude of periastron, ω	~ 0°	323°	18° ± 15°
Standard deviation (km s ⁻¹)	± 21

NOTE.—Hypothetical elements derived from the emission line He II $\lambda 4686$. The period is from Semeniuk 1968.

TABLE 4
PHOTOMETRIC PARAMETERS AND ABSOLUTE DIMENSIONS OF CQ CEPHEI (HD 214419)

A. Photometric Parameters						
PARAMETER	$q = m_2/m_1$					
	0.6	0.7	0.8	0.9	1.0	0.75
$\Sigma = w\sigma^2$	0.242	0.235	0.239	0.231	0.236	0.243
i (degree)	68.63 ± 0.32	68.40 ± 0.33	68.68 ± 0.40	68.54 ± 0.29	67.91 ± 0.24	68.00 ± 0.35
T_2 (K)	41652 ± 442	41750 ± 442	41371 ± 524	40567 ± 738	40800 ± 628	41783 ± 497
$\Omega_1 = \Omega_2$	2.866 ± 0.012	3.037 ± 0.013	3.229 ± 0.013	3.378 ± 0.013	3.496 ± 0.013	3.113 ± 0.017
$L_1/(L_1 + L_2)$ (UV)	0.641 ± 0.014	0.609 ± 0.014	0.586 ± 0.018	0.572 ± 0.027	0.547 ± 0.023	0.595 ± 0.016
$L_1/(L_1 + L_2)$ (yellow)	0.633 ± 0.011	0.603 ± 0.012	0.578 ± 0.010	0.562 ± 0.020	0.538 ± 0.018	0.589 ± 0.013
Ω_{in}	3.063	3.243	3.417	3.586	3.750	3.331
Ω_{out}	2.712	2.842	2.967	3.088	3.207	2.905
$(\Omega_{in} - \Omega)/(\Omega_{in} - \Omega_{out})$	56.1%	51.4%	41.8%	41.8%	46.8%	51.2%
r_1 pole	0.4308 ± 0.0022	0.4180 ± 0.0022	0.4019 ± 0.0020	0.3934 ± 0.0019	0.3897 ± .0019	0.4131 ± 0.0028
r_1 side	0.4645 ± 0.0029	0.4481 ± 0.0029	0.4287 ± 0.0026	0.4192 ± 0.0054	0.4158 ± 0.0025	0.4425 ± 0.0037
r_1 back	0.5121 ± 0.0045	0.4968 ± 0.0046	0.4753 ± 0.0041	0.4680 ± 0.0041	0.4705 ± 0.0043	0.4928 ± 0.0060
r_2 pole	0.3483 ± 0.0023	0.3595 ± 0.0023	0.3651 ± 0.0020	0.3760 ± 0.0019	0.3897 ± 0.0019	0.3659 ± 0.0028
r_2 side	0.3700 ± 0.0029	0.3820 ± 0.0029	0.3873 ± 0.0026	0.3996 ± 0.0054	0.4158 ± 0.0025	0.3892 ± 0.0037
r_2 back	0.4330 ± 0.0060	0.4408 ± 0.0056	0.4489 ± 0.0046	0.4510 ± 0.0043	0.4705 ± 0.0043	0.4479 ± 0.0070
Δm (UV)	0.63 mag	0.48 mag	0.38 mag	0.31 mag	0.20 mag	0.42 mag
Δm (yellow)	0.59 mag	0.45 mag	0.34 mag	0.27 mag	0.17 mag	0.39 mag

B. Absolute Dimensions ^a												
QUANTITY	$q = m_2/m_1$											
	0.6		0.7		0.8		0.9		1.0		0.75	
	N IV	H9	N IV	H9	N IV	H9	N IV	H9	N IV	H9	N IV	H9
$m_1(m_\odot)$	74.6	42.5	62.1	35.4	41.5	23.6	31.2	17.7	25.5	14.5	46.3	26.4
$m_2(m_\odot)$	44.7	25.6	43.4	24.7	33.2	18.9	28.1	16.0	25.5	14.5	34.7	19.8
$a(R_\odot)$	28.8	23.9	26.3	21.8	24.3	20.1	22.8	18.9	21.7	18.0	25.3	21.0
$R_1(R_\odot)$	13.4	11.1	11.8	9.8	10.4	8.6	9.6	8.0	9.0	7.5	11.2	9.3
$R_2(R_\odot)$	10.7	8.9	10.0	8.3	9.4	7.8	9.1	7.5	9.0	7.5	9.8	8.1

NOTE.—This table assumes $T_1 = 45,000$ K. Component 1 = WN7 star; component 2 = O6 star.

^aN IV means values based on N IV $\lambda 4058$ in emission and H9 means H9 $\lambda 3835$ in absorption.

by Niemela (1980). However, its present amplitude $K \approx 150 \text{ km s}^{-1}$ is quite different from Niemela's (1980) $K \approx 340 \text{ km s}^{-1}$. Also, it would be highly unusual for an O-star to display such a strongly violet displaced He I component.

IV. PHOTOMETRIC SOLUTIONS AND ABSOLUTE DIMENSIONS

The 1947 photoelectric observations of CQ Cep by Hiltner (1950) were utilized in our analysis. There were

382 and 188 observations in yellow and in ultraviolet, respectively. We applied a correction of $0^{\text{d}}020$ in phase (Hiltner 1950, Tables 3 and 4), as was suggested at the end of his paper. It was assumed that Hiltner's period probably gives the best representation to his results; therefore, we employed his period and light curves as they were. Since the observing intervals of Hiltner's (1950) photometric data and the present spectroscopic data are short, any small difference in period is irrelevant. Hiltner (1950) detected significant variation in the

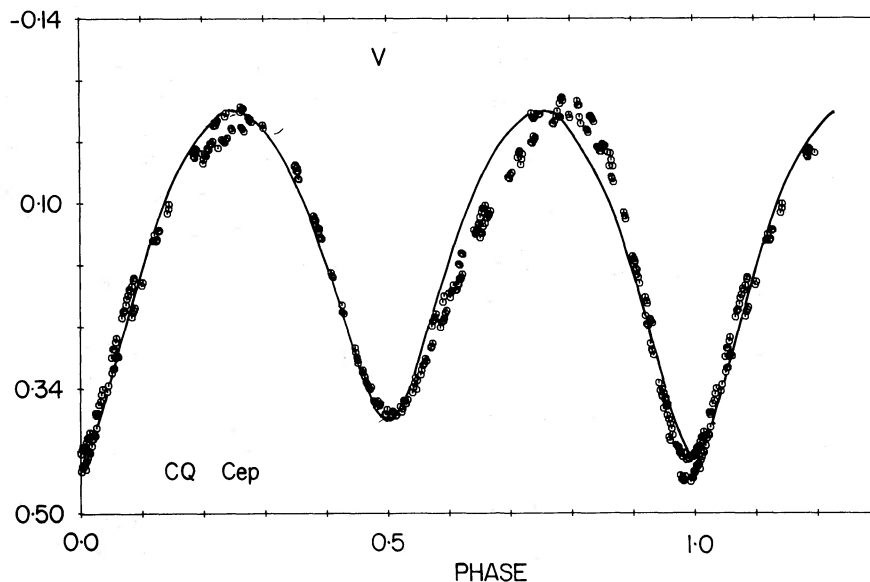


FIG. 6.—The 1947 yellow light curve of CQ Cep. Circles denote Hiltner's 1950 observations. The smooth curve represents the computed light curve for mass ratio $q = 0.75$.

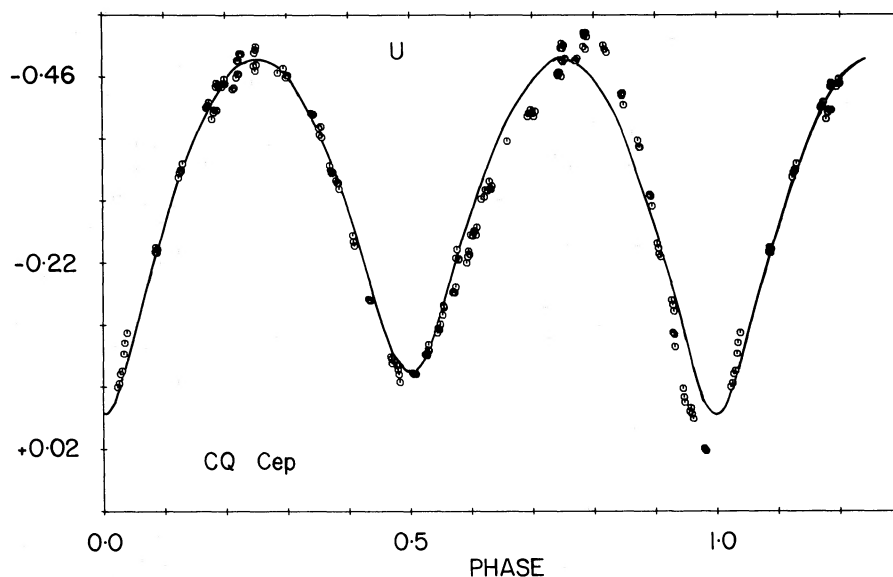


FIG. 7.—The 1947 ultraviolet light curve of CQ Cep as in Fig. 6

light curves from one epoch to another and published both the observed and "smoothed" magnitudes (by applying different corrections to the observations made at different epochs). In our analysis, we employed only the observed magnitudes. Even though the scatter is greater in the observed light curves (Figs. 6 and 7 compared with the smoothed light curves of Hiltner, Figs. 1 and 2), they represent the true light variations of the binary system CQ Cep.

There are large asymmetries in the light curves (see Hiltner 1950 for details). In view of these asymmetries, CQ Cep is reminiscent of the massive contact binary UW CMa (Leung and Schneider 1978), where the secondary maximum (Max II) occurs at phase 0.77 (this occurs at phase 0.80 in CQ Cep). UW CMa (period $P = 4.4$) has a spectral type of O7f Ia+0, whereas CQ Cep has a spectral type of WN7+O (Smith 1968). It seems that in going from an Of system to a WN7 system ("transition system," Conti 1975), the asymmetry becomes more pronounced. This suggests that the mass-flow activity in a W-R system is even more dramatic than in an Of system. However, the degree of overcontact may also play a role.

As in the case of UW CMa, it is impossible to fit the whole light curve with a normal binary model without invoking some feature of inhomogeneous mass-flow, star spots, or similar. We employed the 1977 version (Leung and Wilson 1977) of the Wilson and Devinney (1971) computing code for circular orbits. The asymmetries and the unequal durations of the light curve minima are likely caused by the nonuniform surface brightness of the system and are probably not the result of a possible orbital eccentricity. After a few trials, it was discovered that the asymmetry of the light curve over the range of phases ~ 0.5 to ~ 1.0 does not allow a good fit with normal binary models. At this point, the following assumptions were thus made: (1) We anchored the light curve at the secondary minimum, i.e., shifted Min II to phase 0.50, exactly, allowing Min I to differ from phase 0.0; (2) omitted the observations between phases 0.57 and 1.00 from our analysis. Note that a similar approach was applied to UW CMa (Leung and Schneider 1978). Initially a detached configuration, mode 2 (see Leung and Wilson 1977 for discussion of modes), was fitted, but it was soon realized that the system CQ Cep has a contact configuration. Thus, we proceeded to derive our model with mode 3 (contact) configuration. It was then obvious to us that this complex system does not allow a unique solution, especially with respect to the mass ratio $q = m_2/m_1$. (We recall that m_1 is the mass of the WN7 star, i.e., the component eclipsed at the primary minimum.) Consequently, series of photometric parameters were obtained with several assumed values of q ; they are listed in Table 4.

All values are based on the effective temperature $T_1 = 45,000$ K, a reasonable compromise for WN7 (Conti 1979; Leep 1979; Willis and Wilson 1979) and close to

the temperature adopted for the primary of component of UW CMa.

The sums of the weighted square-deviations ($\sum w\sigma^2$ in Table 4A) are about the same for all assumed values of q . Therefore, the computed light curves from different solutions are indistinguishable in graphs of small scale. The computed light curves in yellow and in ultraviolet with $q = 0.75$ are plotted along with the observations in Figures 6 and 7, respectively. The yellow observations show significant systematic nightly variations. The asymmetry between about phases 0.5 and 1.0 cannot be reproduced by the model (computed light curve). This complication can also be seen in Hiltner's (1950, Fig. 4) He II $\lambda 4686$ photometry and in the unusually small radial velocity amplitude of He II $\lambda 4686$ in our Figure 4. These suggest enormous activity during this phase.

A graphical comparison of selected parameters derived from different assumed values of q is shown in Figure 8. Inspection of the first two plots in the upper part of the diagram leads to the conclusion that the inclination i and the temperature T_2 of the secondary

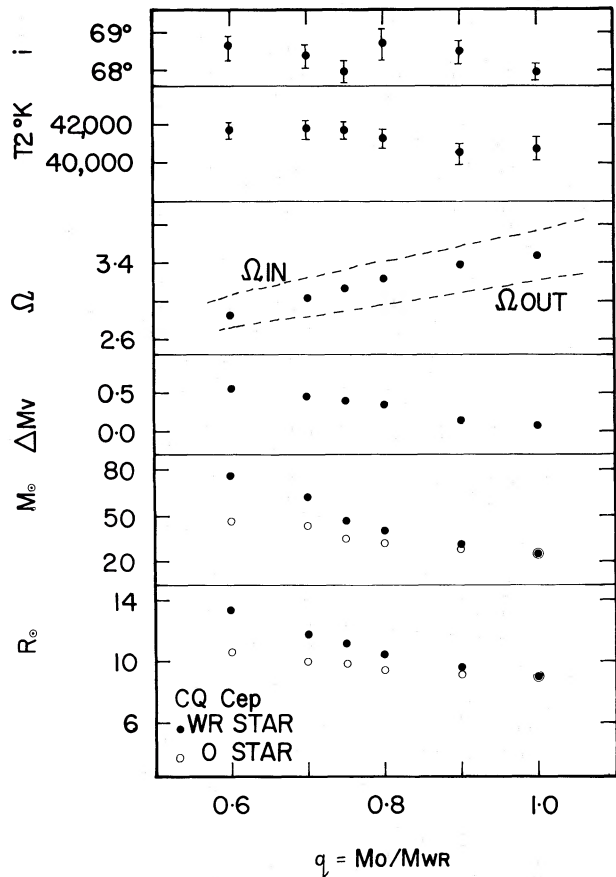


FIG. 8.—The photometric parameters and the derived quantities vs. the assumed values for the mass ratio q of CQ Cep.

component (or the difference in temperature between the components) are very well determined. In the third plot of Figure 8, we see that the system remains in contact configuration for the values of q plotted, and the degree of overcontact stays constant within $\pm 5\%$ of the mean. The other parameters, relative radii and luminosities, are functions of q , as to be expected.

From the luminosities, one can calculate the magnitude difference Δm . This quantity is very sensitive to q as shown in the fourth plot of Figure 8. Δm_v increases from 0.0 mag to 0.6 mag for q decreasing from 1.0 to 0.6, respectively. If $\Delta m \approx 0.4$ mag, this means that the absorption lines of the unseen O-type star (O6, according to T_2 with assumed $T_1 = 45,000$ K) must be $\sim 50\%$ less deep than the absorption lines of the WN7 component, assuming that the sets of absorption lines of both stars are intrinsically about the same. This should make the O type star marginally detectable. The equatorial rotational velocity of both stars for synchronous rotation (see below) is ~ 300 km s $^{-1}$. This would make the absorption lines even broader and shallower. Under this condition, we believe that if $\Delta m \geq 0.4$ mag, the O type star would be either extremely difficult to detect or in fact undetectable. It is still debatable whether the spectrum of the O type star has been seen. Our spectra do not show absorption in antiphase with emission, unlike those claimed for He II $\lambda 4686$ and He I $\lambda 3889$ by Niemela (1980). Therefore, this limit leads to $q \leq 0.75$.

Absolute dimensions of a binary system can be obtained from the combined results of photometry and spectroscopy. The velocity amplitude (semiamplitude) of CQ Cep (Table 2) depends on the spectral line used. In view of its moderate strength and symmetry, the most reliable emission line to reflect the orbit is probably N IV $\lambda 4058$; the only reliable absorption line is that of H9 $\lambda 3835$. These two lines also come close to representing the two extremes in velocity amplitude, 310 and 257 km s $^{-1}$, respectively. It is not obvious which of these two lines best represents the true orbit, if at all. As already stated, the Balmer absorption appears to be formed in an accelerating photosphere (mean velocity of H9: $\gamma = -261$ km s $^{-1}$) on the line of sight from the star to the observer; thus, it may be sensitive to local wind perturbations. The N IV emission arises probably in a more extended zone around the WN7 star and is possibly more sensitive to perturbations of the wind by the companion O type star. However, in this case, the line should be less affected *overall* since we see it arising from a larger volume of the wind where local perturbations are possibly more smeared out. Its γ -velocity (-60 km s $^{-1}$) matches well the radial component expected from galactic rotation, unlike the other emission lines (see § III). The absolute dimensions of the binary system as a function of the mass ratio q are given in Table 4B (employing N IV $\lambda 4058$ and H9) and plotted in the lower part of Figure 8 (where only N IV values are employed). The mass and radius increase rapidly as q

decreases. In the case of the N IV $\lambda 4058$ emission line, the mass of the WN7 component reaches $80 m_\odot$ for $q = 0.6$! If we accept that WN7 stars have masses ranging from $\sim 25 m_\odot$ to at most $\sim 50 m_\odot$ (Massey 1981), the limit of the mass ratio will be $q \geq 0.70$. By combining this constraint with the limit set by the magnitude difference discussed earlier, the true mass ratio is most likely in the range $0.70 \leq q \leq 0.75$.

If we let $q = 0.75$, the rotation velocity $v \sin i$ derived from the period and the radius (assuming synchronized rotation as the likely case for a contact system) is about 320 km s $^{-1}$ for the WN7 component. The estimated widths at the bases of the absorption lines H9, He II $\lambda 4200$, H γ , and He II $\lambda 4542$ are 7.6, 8.7, 9.8, and 8.7 Å, respectively. These lead to a mean $v \sin i$ of 310 ± 11 km s $^{-1}$. Thus, the value of $v \sin i$ derived for $q = 0.75$ compares very well with the observed value.

V. INTERPRETATION OF CQ CEPHEI

Even though the light curves and radial velocity curves are very complicated, we have narrowed the solution to a very small range around $q = m_2/m_1 = m_O/m_{WN7} \approx 0.75$. The configuration of CQ Cep for this solution is shown in Figure 9. The unbracketed and bracketed values represent the absolute dimensions derived from N IV $\lambda 4058$ and H9, respectively. The system lies about halfway between the inner and the outer contact surfaces. The direction of binary revolution is denoted by the curved arrows. The direction of the line of sight at phase 0.8 is indicated by an arrow pointing to the center of gravity and labeled $p = 0.8$. We believe this to be the "hot" region or the region of enhanced outflowing mass-flow from the W-R component. This active region is responsible for making the Max II brighter than Max I and also shifting its maximum to phase 0.8. The excess mass-flow region is located in the lagging surface of the hotter component with respect to its binary motion. This fits into the general scheme for a dynamical model.

It is noted that the simplified binary model, which neglects nonuniform surface brightness variations, only represents the "best fit" to the light curve. Until more is known about such asymmetries, we can only assume that they affect only a portion of the light curve, not the whole. Thus, the parameters derived still probably represent a fairly reliable estimate of the binary system.

The radial velocity amplitude increases from lower values for the absorption lines to higher values for emission lines (Table 2). The reason for this is not clear. This tendency breaks down for the emission He II $\lambda 4686$ which has *lower* velocity amplitude; this effect is typical for WNL binaries of short period (A. F. J. Moffat, unpublished). Possibly, this is related to the ejection of hot, $\lambda 4686$ emitting material with a strong RV component directed toward the observer around phase 0.8 (cf. Fig. 9); this will reduce the net RV amplitude of this line (cf. Fig. 4). Note that in other single or long-period

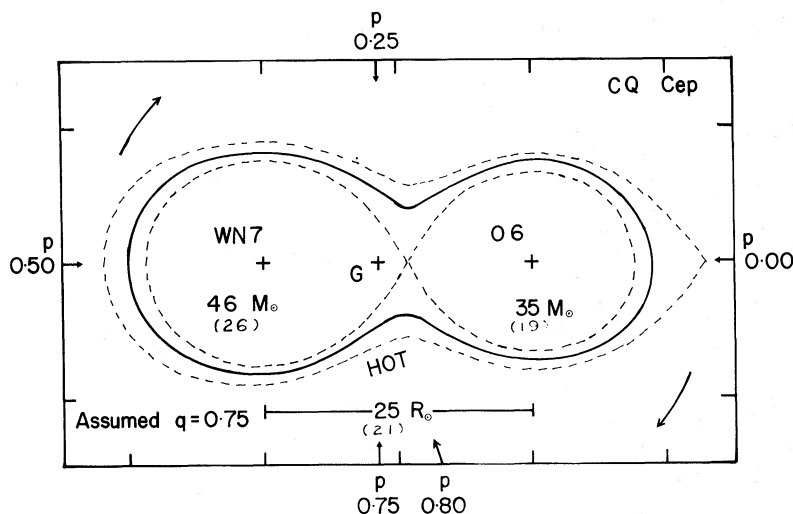


FIG. 9.—The configuration of CQ Cep (WN7+O6) in the orbital plane for mass ratio $q = 0.75$. The center of gravity G is marked by a plus sign; the phases of orbital motion are denoted by p . The unbracketed and bracketed values represent the masses and distance of the stellar centers derived from the N IV $\lambda 4058$ and H9 $\lambda 3835$ radial velocity curves, respectively. Phase $p = 0.80$ points to the active region of the binary.

binary WNL stars, He II $\lambda 4686$ has a considerably more positive mean RV than N IV $\lambda 4058$. In CQ Cep this effect becomes diminished around phase 0.8. The fact that maximum He II $\lambda 4686$ emission strength occurs at phases 0.0 and 0.5 (Hiltner 1950) must be the result of further geometrical effects, possibly related to Roche lobe geometry.

VI. CONCLUSIONS

Unlike most W-R binaries of lower luminosity (early WN, WC), the single-line eclipsing binary CQ Cep contains a luminous WN7 component whose mass exceeds that of its presumed O type companion. The presence of hydrogen in the W-R envelope, as clearly seen from the alternating Pickering decrement, implies that CQ Cep has either not yet peeled off enough of its outer layers to reveal He-rich, processed matter or it is a very massive star still in the stage of core H-burning (cf. de Loore, De Grève, and Vanbeveren 1978; Chiosi, Nasi, and Bertelli 1979).

CQ Cep is the shortest period W-R binary known. The radius of the WN7 photosphere is $\sim 11 R_{\odot}$ and certainly lies between 9 and $13 R_{\odot}$ (cf. Table 4). This was derived assuming $T_1 = 45,000$ K. If we take a lower value like $T_1 = 26,000$ K (cf. Underhill 1981), the de-

rived radius does not change significantly. This is in stark contrast with the mean radii of WN7/8 stars given by Underhill (1981): $33 R_{\odot}$, based on observed fluxes from IR to UV. Noting that $45,000^4 \times 11^2 = 26,000^4 \times 33^2$, we draw two possible conclusions: either CQ Cep is a peculiar object or Underhill's (1981) radii and effective temperatures for WN7/8 stars are invalid. Clearly, one needs more direct information on the geometrical dimensions of W-R stars.

Finally, we draw attention to a recently received preprint by Stickland *et al.* (1982) which combines data from the far-UV to the IR. In particular, they derive a relatively large effective radius for the W-R component ($17.5 R_{\odot}$) such that the O-star passes well within it. The ensuing bow shock is then claimed to account qualitatively for the observations. The true nature of CQ Cep possibly lies somewhere between their and our models.

K. C. L. is supported in part by a University of Nebraska Research Council Grant. A. F. J. M. is grateful to the Natural Sciences and Engineering Research Council of Canada for financial aid. Part of the reduction was carried out by W. S. with an efficient desk computer granted by the Deutsche Forschungsgemeinschaft (grant Schm 167/12).

REFERENCES

- Bappu, M. K. V., and Visvanadham, P. 1977, *Kodaikanal Obs. Bull., Ser. A*, **2**, 89.
 Chiosi, C., Nasi, E., and Bertelli, G. 1979, *Astr. Ap.*, **74**, 62.
 Conti, P. S. 1975, *Mém. Soc. R. Sci. Liège*, Ser. 6, **9**, 193.
 ———, 1979, in *IAU Symposium 83, Mass Loss and Evolution of O-Type Stars*, ed. P. S. Conti and C. W. H. de Loore (Dordrecht: Reidel), p. 431.
 Conti, P. S., Niemela, V. S., and Walborn, N. R. 1979, *Ap. J.*, **228**, 206.
 de Loore, C., De Grève, J. P., and Vanbeveren, D. 1978, *Astr. Ap.*, **67**, 373.
 Gaposchkin, S. 1944, *Ap. J.*, **100**, 242.
 Gusseinzade, A. A. 1969, *Perem. Svezdy*, **16**, 488.
 Hiltner, W. A. 1944, *Ap. J.*, **99**, 273.

- Hiltner, W. A. 1950, *Ap. J.*, **112**, 477.
 Hiltner, W. A., and Schild, R. E. 1966, *Ap. J.*, **143**, 970.
 Kartasheva, T. A. 1972, *Perem. Zvezdy*, **18**, 459.
 ———. 1976, *Pis'ma Astr. Zh.*, **2**, 505; also *Soviet Astr. Letters*, **2**, 197.
 Kartasheva, T. A., and Svechnikov, M. A. 1974, *Perem. Zvezdy*, **19**, 441.
 Khaliullin, Kh. F. 1972, *Astr. Zh.*, **49**, 777; also *Soviet Astr. J.*, **16**, 636.
 Khaliullin, Kh. F., and Cherepashchuk, A. M. 1970, *Astr. Tsirk.*, No. 551, 5.
 Leep, E. M. 1979, in *IAU Symposium 83, Mass Loss and Evolution of O-Type Stars*, ed. P. S. Conti and C. W. H. de Loore (Dordrecht: Reidel), p. 471.
 Leung, K. C., and Schneider, D. P. 1978, *Ap. J.*, **222**, 924.
 Leung, K. C., and Wilson, R. E. 1977, *Ap. J.*, **211**, 853.
 Massey, P. 1981, *Ap. J.*, **246**, 153.
 McLaughlin, D. B., and Hiltner, W. A. 1941, *Pub. A.S.P.*, **53**, 328.
 Moffat, A. F. J., and Seggewiss, W. 1977, *Astr. Ap.*, **54**, 607.
 Moffat, A. F. J., 1978, *Astr. Ap.*, **70**, 69.
 ———. 1979, *Astr. Ap.*, **77**, 128.
 Niemela, V. S. 1980, in *IAU Symposium 88, Close Binary Stars: Observations and Interpretation*, ed. M. J. Plavec, D. M. Popper, and R. K. Ulrich (Dordrecht: Reidel), p. 177.
 Semeniuk, I. 1968, *Acta Astr.*, **18**, 313.
 Smith, L. F. 1968, *M.N.R.A.S.*, **138**, 109.
 Stickland, D. J., Burton, W. M., Bromage, G., Willis, A. J., Howarth, I. D., Budding, E., and Jameson, R. F. 1982, preprint.
 Tchugainov, P. F. 1960, *Perem. Zvezdy*, **13**, 148.
 Underhill, A. B. 1969, in *Mass Loss from Stars*, ed. M. Hack (Dordrecht: Reidel), p. 17.
 ———. 1981, *Ap. J.*, **244**, 963.
 Willis, A. J., and Wilson, R. 1979, in *IAU Symposium 83, Mass Loss and Evolution of O-Type Stars*, ed. P. S. Conti, and C. W. H. de Loore (Dordrecht: Reidel), p. 461.
 Wilson, R. E., and Devinney, E. J. 1971, *Ap. J.*, **166**, 605.
 Wilson, R. E., and Sofia, S. 1976, *Ap. J.*, **203**, 182.

KAM-CHING LEUNG: Department of Physics and Astronomy, Behlen Laboratory of Physics, University of Nebraska, Lincoln, NE 68588

ANTHONY F. J. MOFFAT: Département de Physique, Université de Montréal, C.P. 6128, Succ. "A," Montréal, Québec H3C 3J7, Canada

WILHELM SEGGEWISS: Observatorium Hoher List, Universität Bonn, D-5568 Daun, Federal Republic of Germany